Frontiers in Bioscience Landmark

Front. Biosci. (Landmark Ed) **2023**; 28(4): 82
https://doi.org/10.31083/j.fbl2804082

Original Research

Polysaccharides of *Floccularia luteovirens* Alleviate Oxidative Damage and Inflammatory Parameters of Diabetic Nephropathy in db/db Mice

Huan Wang[1,2,†], Yang Yang[1,3,†], Shumin Wang[2], Changtian Li[1], Changbao Chen[2], Xilin Wan[2], Dan Li[1,*], Yu Li[1,*]

[1]National-Local Joint Engineering Research Center of Economic Fungus, Jilin Agricultural University, 130118 Changchun, Jilin, China
[2]Jilin Ginseng Academy, Changchun University of Chinese Medicine, 130117 Changchun, Jilin, China
[3]Environment and Plant Protection Institute, Chinese Academy of Tropical Agricultural Sciences, 571101 Haikou, Hainan, China
*Correspondence: lidan@ jlau.edu.cn (Dan Li); yuli966@126.com (Yu Li)
[†]These authors contributed equally.

Academic Editors: Luciano Saso, Grzegorz Wegrzyn and Hande Gurer-Orhan
Submitted: 6 October 2022 Revised: 20 December 2022 Accepted: 27 December 2022 Published: 27 April 2023

Abstract

Background: *Floccularia luteovirens* (Alb. & Schwein.) Pouzar, is an extremely rare edible and medicinal mushroom in China. The crude polysaccharides of *F. luteovirens* (FLPs) has significant antioxidant and anti-inflammation activities and exerts excellent protective functions in diabetic nephropathy (DN) complications, but the material basis of the pharmacological effects of FLPs and the molecular mechanism of its pharmacological action are still unclear. **Methods**: First, we performed systemic composition analysis on extracted and isolated FLPs. Next, the spontaneous db/db mouse DN model was used to investigate the mitigation and protection functions of FLPs in DN and the underlying mechanism through the mammalian target of the rapamycin (mTOR)/GSK-3β/NRF-2 pathway. **Results**: FLPs contained 65.0% total sugars, 7.2% reducing sugars, 7.93% proteins, 0.36% total flavonoids, 17 amino acids, 13 fatty acids, and 8 minerals. After intragastric administration of FLPs with concentrations of 100, 200 and 400 mg/kg for 8 weeks, FLPs inhibited excessive weight gain, relieved the symptoms of obesity, and significantly improved glucose metabolism and lipid metabolism in the db/db mice. In addition, FLPs were also involved in regulating the indicators of various oxidases and inflammatory factors in the serum and kidney of db/db mice. **Conclusions**: FLPs effectively improved and relieved kidney tissue injury caused by high glucose, targeted and regulated phospho-GSK-3β, and suppressed inflammatory factor accumulation. Furthermore, FLPs activated the nuclear factor erythroid 2-related factor 2/heme oxygenase 1 (NRF2/HO-1) pathway and enhanced the activity of catalase (CAT) to further play a role in relieving and treating T2DM and nephropathy complications.

Keywords: *Floccularia luteovirens*; diabetic nephropathy; fungal polysaccharide; oxidative stress; inflammation

1. Introduction

Diabetes mellitus (DM), a chronic metabolic disorder characterized primarily by persistent hyperglycemia and abnormal blood lipids, affects tissues and organs throughout the body [1]. The number of DM patients in China is the highest in the world, and DM has become one of the world's most serious and critical health issues [2–4]. The deleterious effects of diabetes are reflected in a variety of long-lasting complications that are difficult to cure, and diabetic nephropathy (DN) has become one of the most important factors influencing the high morbidity and mortality rate for DM [5]. Among DM patients, the incidence of DN is 30–40% [1]. DN is a common and serious complication of chronic microvascular disease, and can cause end-stage renal and chronic kidney disease (ESRD) [6].

The pathogenesis of DM and its complications is complex and diverse. Increasing evidence indicates that oxidative stress is a crucial mechanism in the development of DM. Oxidative stress and inflammation are important factors that regulate and influence the occurrence and development of DN. There is a strong connection between oxidative stress and inflammation, as they influence and promote each other [7]. DN-related oxidative stress is caused by an increase in reactive oxygen species (ROS) and a decrease in antioxidant activity in the body. The oxidative stress is mainly induced by disruption of activation of the transcription nuclear factor erythroid-2 related factor 2 (NRF2). NRF2 is a redox-sensitive transcription factor, which plays an important protective role in regulating the physiological responses to oxidative stress in the body by regulating genes that encode phase-II detoxifying enzymes and antioxidant proteins. By targeting NRF2, cell protective genes associated with the antioxidant response are activated to inhibit oxidative stress and inflammatory responses. Glycogen synthase kinase 3β (GSK-3β), a typical serine/threonine kinase, is abundantly expressed in many organs of the body. It is involved in the regulation of NRF2 in many conditions and diseases, such as aging, type 2 DM, neurological, and liver diseases [8]. In the NRF2 noncanonical regulatory response, i.e., the Keap1-independent signaling pathway, GSK-3β is considered a "common effector" of many NRF2 inducers and is the major mechanism by which NRF2

is regulated after cell stimulation. GSK-3β can mediate the nuclear export and degradation of nuclear NRF2 to negatively regulate the NRF2 signaling pathway [9,10]. Therefore, NRF2 may provide a new therapeutic target for DN treatment and it has been a notable target in recent studies of DM and related complications [11]. Several recent studies have also confirmed the efficacy of NRF-2/HO-1 in the treatment of DN [12–14].

There is currently no safe and ideal therapeutic drug for DM and DN. Therefore, early therapeutic measures targeting DM and DN are needed to develop preventive and therapeutic drugs that are stable, highly effective, and widely available and have low toxic side effects. Fungal polysaccharides have excellent biological activities, such as lowering blood sugar, and antioxidant, anti-inflammatory, and antitumor properties [15,16], and have become a focus of the pharmaceutical and food industries. *Floccularia luteovirens* (Alb. & Schwein.) Pouzar, also known as *Armillaria luteovirens*, is referred to throughout China as "Qilian yellow mushroom". It belongs to the Basidiomycota, Agaricomycotina, Agaricomycetes, Agaricales, Agaricaceae, *Floccularia species* [17,18]. It grows in summer and autumn on grasslands or alpine meadows at an altitude of 2500–4800 m and usually forms mycorrhiza with Kobresia plants [19]. It is mainly distributed in Qinghai, Tibet, and Sichuan. In addition, it is also distributed in other provinces such as Hebei, Shaanxi and Gansu [18,20].

Our previous studies involved exploratory investigations of the anti-type 2 DM activities of water extract of *Floccularia luteovirens* (FLW) and crude polysaccharides of *Floccularia luteovirens* (FLPs). The results indicated that FLW and FLPs had significant antioxidant and antiinflammation activities and exerted excellent protective functions in DN complications [21,22]. However, the pharmacological effects of FLPs and the molecular mechanism of their pharmacological actions are still unclear, and both need to be further studied.

First, we performed systemic composition analysis on extracted and isolated FLPs. Next, the spontaneous db/db mouse DN model was applied to investigate the mitigation and protection functions of FLPs on DN and the underlying mechanism through the mammalian target of rapamycin (mTOR)/GSK-3β/NRF-2 pathway to provide theoretical bases for the development of natural, safe, and effective anti-DM functional foods and drugs.

2. Materials and Methods

2.1 Extraction and Separation of FLPs

The fruiting bodies of *F. luteovirens* were collected from Sêrxü County of Ganzi Autonomous Prefecture in Sichuan Province and identified by Professor Yu Li. The specimen was stored in the Herbarium of Mycology of Jilin Agricultural University (HMJAU) under specimen number HMJAU44964.

Fruiting bodies were placed in a drying oven, dried at 55 ℃ to a constant weight, crushed, and passed through an 80-mesh sieve. After degreasing with petroleum ether and 95% ethanol, crude polysaccharides were extracted using the classic water-extraction and alcohol-precipitation method [23,24]. After the majority of proteins were removed using the papain enzyme-Sevag method, FLPs were obtained after dialysis (mw cutoff: 3500 Da) and lyophilization. The detailed extraction procedures are shown in Fig. 1.

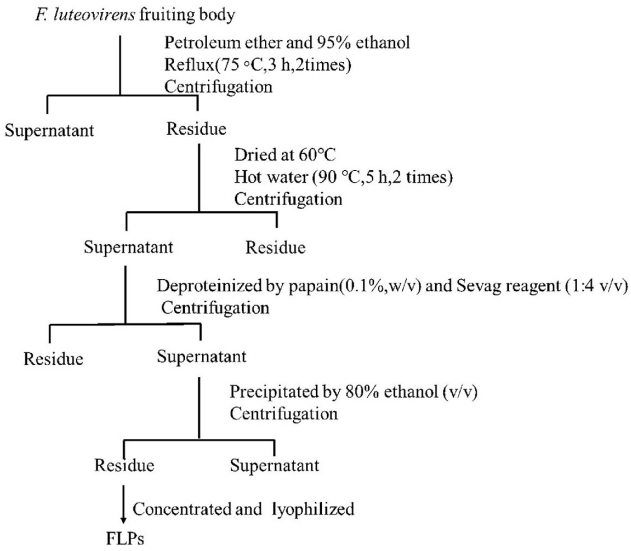

Fig. 1. Extraction and isolation of FLPs.

2.2 Measurement of FLPs Components

In this study, we used the phenol-sulfuric acid method [25], direct titration method [26], Kjeldahl determination (UDK169, VELP, Italy) [27], UV spectrophotometry [28], and periodate oxidation method [29] to analyze the levels of total sugars, reducing sugars, proteins, total flavonoids, and mannitol in FLP samples. The hydrolyzed amino acids in FLPs were determined by an automatic analyzer (Hitachi L-8900, Kyoto, Japan). The fatty acid levels were analyzed by the Gas chromatography mass spectrometry method (QP2010, Shimadzu, Kyoto, Japan) [30]. The mineral elements were analyzed using inductively coupled plasma optical emission spectrometry (ICP-OES) (Varian 720-ES, Varian, Palo Alto, CA, USA) and inductively coupled plasma mass spectrometry (ICP-MS) (BRUKER aurora M90, MA, USA) [30,31].

2.3 Animal Experimental Procedure

Eight-week-old male db/m+ and db/db grade mice without specific pathogens (SPF) were provided by the Biomedical Research Institute of Nanjing University. The license of experimental animals was SCXK (Su) 2015-0001. The feeding temperature of the experimental animals was 23 $\pm$ 1 ℃, the relative humidity was 55 $\pm$ 5%,

and the light-dark alternating time was 12 h. Animals were easily able to get food and water. All experiments were carried out in strict accordance with the Regulations on the Use of Experimental Animals and the China Animal Welfare Law, and were approved by the Experimental Animal Ethics Committee of Changchun University of Traditional Chinese Medicine.

After 1 week of adaptive feeding, all animals were used for experiments. A total of 10 db/m+ mice were considered as the controls (CK). The db/db mice with blood glucose >11.1 mmol/L were divided into 5 groups, 10 in each group. Drug administration was performed for 8 weeks, and the weight and blood glucose were measured weekly. The specific drug administration regimens were as follows: (a) model group–treatment with an equal volume of normal saline, n = 10; (b) positive control group – treatment with 0.10 g/kg metformin (Met) hydrochloride, n = 10; (c) low-dose group–treatment with FLP solution at 100 mg/kg, n = 10; (d) middle-dose group–treatment with FLP solution at 200 mg/kg, n = 10; (e) high-dose group–treatment with FLP solution at 400 mg/kg, n = 10; and (f) normal control group–treatment with an equal volume of normal saline, n = 10.

2.4 Oral Glucose Tolerance Test (OGTT)

After drug administration for 8 weeks, db/db mice were fasted overnight (at least 12 h) after the last drug administration, drank water freely, and a OGTT was then performed. The weights and fasting blood glucose levels in mice were gauged. Mice in each group received intragastric administration of 2.0 g/kg glucose solution, and blood samples were obtained from the tail vein at 0, 30, 90, 120 and 240 minutes after intragastric administration to measure blood glucose levels. The area under the curve (AUC) of glucose was assessed by the trapezoidal method [32]: AUC = (blood glucose value at 0 min + blood glucose value at 30 min) $\times$ 0.25 + (blood glucose value at 30 min + blood glucose value at 60 min) $\times$ 0.25 + (blood glucose value at 60 min + blood glucose value at 120 min) $\times$ 0.5.

2.5 Sample Collection and Detection of Biochemical Indicators

Serum collection: After 8 weeks of drug administration, mice were fasted for 12 h and drank freely. Blood specimens were collected from the retroorbital plexus and centrifuged rapidly for 10 min (3000 rpm). The supernatant was aspirated, and mouse serum specimens were obtained. For collection of organs: mice were sacrificed by cervical dislocation and rapidly dissected. Kidney, spleen, and liver tissues were collected and weighed. The remaining tissues were fixed in 4% paraformaldehyde or stored in a –80 °C freezer for future use.

Glutathione peroxidase (GSH-Px), superoxide dismutase (SOD), catalase (CAT), high-density lipoprotein cholesterol (HDL-C), low-density lipoprotein cholesterol (LDL-C), triglyceride (TG) and total cholesterol (TC) levels in serum samples were measured with ELISA kits. In addition, SOD, CAT, GSH-Px, ROS, tumor necrosis factor-α (TNF-α), N-acetyl-β-D-glucosaminidase (NAG), interleukin-2 (IL-2), IL-6, interleukin-1β (IL-1β), interferon-α (IFN-α), IFN-γ, NF-κB, and matrix metallopeptidase 9 (MMP-9) levels in kidney tissue were also measured.

2.6 Renal Histopathology

The 4% paraformaldehyde was used to fix spleen and kidney tissues. After dehydration, paraffin was used for kidney tissues embedding, then cut into slices (thickness of approximately 5 μm), deparaffinized, subject to staining with periodic acid-Schiff (PAS) and hematoxylin-eosin (H&E), mounted, and observed under a microscope for pathological changes in kidney tissues.

2.7 Western Blot Analysis

The RIPA protein lysis buffer solution containing 1% protease inhibitor cocktail (cocktail P8340, Sigma-Aldrich, USA) and 2% PMSF (phenyl methyl sulfonyl fluoride) (P7626, Sigma-Aldrich, USA), which stored at low temperature for 10 minutes, were used to extract total protein from an appropriate amount of kidney tissue. After centrifugation, the protein content in supernatant was measured using the bicinchoninic acid protein assay kit (Merck Millipore, Darmstadt, Germany). Loading buffer was added into the protein sample. After denaturation at 95 °C for 5 min, the specimens were aliquoted and storaged at –40 °C. For all specimens, 40 μg was loaded. The gel was removed, and proteins were transferred onto a membrane at a low temperature for 120 min. The membrane was blocked in 5% BSA (A9647, Sigma-Aldrich, St. Louis, MO, USA) at 4 °C for 4 h. The blocked polyvinylidene fluoride or polyvinylidene difluoride (PVDF) membrane was incubated with antibody, and the protein bands were visualized (UVP, Upland, CA, USA) [30]. Changes in protein expression of glyceralde-hyde-3-phosphate dehydrogenase (GAPDH), phosphor (P)-mTOR (S2448, ab109268; Abcam, Cambridge, MA, USA), total (T)-mTOR (ab83495; Abcam, Cambridge, MA, USA), P-GSK-3β (Y216, ab75745), T-GSK-3β (PK1111; Merck Millipore, Burlington, MA, USA), NRF2 (bs-1074R; Bioss, Beijing, China), CAT (ab52477), and HO-1 (ab137749) in mouse kidney tissue were assessed.

2.8 Statistical Analysis

The results data were expressed as mean $\pm$ standard deviation (SD). The differences between groups were compared by ANOVA method in IBM SPSS 22.0 (IBM Corp., Armonk, NY, USA). Figures were plotted using GraphPad Prism 5.0 (GraphPad Software, San Diego, CA, USA).

3. Results

3.1 Composition of FLPs

Systemic composition analysis of the chemical composition of the FLPs samples indicated that FLPs comprised 65.0% total sugars, 7.2% reducing sugars, 7.93% proteins, and 0.36% total flavonoids, whereas mannitol was not detectable (Table 1). FLPs contained 17 types of amino acids including lysine at 0.949%, phenylalanine at 0.837%, glutamic acid at 0.753%, and aspartic acid at 0.674% (Table 2). The levels of 35 types of fatty acids in FLPs were measured, and the results indicated that FLPs contained 13 types of fatty acids (‰), such as oleic acid (43.50), palmitic acid (35.97), linoleic acid (25.47), stearic acid (13.19), elaidic acid (3.69) and arachidonic acid (2.48) (Table 3). FLPs contained 8 mineral elements. Potassium (K), calcium (Ca), and cupper (Cu); heavy metals were not detected (Table 4).

Table 1. Main components of FLPs.

Compounds	Contents (%)
Total sugar	65.00
Reducing sugar	7.20
Total protein	7.93
Flavonoids	0.359
Mannitol	ND①

ND①: not detected (the detection limit was 0.1 g/100 g).

3.2 Hypoglycemic Effects of FLPs

Compared with db/m+ mice, the body weight of untreated db/db mice was approximately 2–3 times higher and showed a significantly increasing trend; in addition, the fasting blood glucose level significantly increased, and liver, spleen, and kidney indicators significantly decreased ($p < 0.001$, Table 5). After Met and FLPs administration in the positive control group for 8 weeks, mouse weights in Met group and FLPs drug administration groups had different levels of reduction compared with the model (db/db) group; however, their differences were not significant. The administration of FLPs (100 mg/kg) generated significant inhibitory effects on body weight during the last 4 weeks ($p < 0.001$) (Table 5), indicating that FLPs inhibited excessive increases in mouse body weight and relieved obesity symptoms in db/db mice to some extent. Significant hypoglycemic effects were observed in the FLPs (200 mg/kg) drug administration group starting from week 6 ($p < 0.05$, Table 5). The results showed that FLPs did not have significant effects on mouse liver and spleen indicators after 8 weeks of drug administration in the model group but significantly elevated the kidney indicators in model group (Table 5). Therefore, this research showed FLPs did not have toxic side effects on organs and generated certain improvements in kidney indicators in db/db mice.

One-hour plasma glucose (1-h PG), an accurate predictor of type 2 DM [33]. OGTTs were conducted in the mice in all groups. Fasting blood glucose levels at 0 min were measured first. After the intragastric administration of 2.0 g/kg glucose solution, the levels of glucose in all groups began to significantly increase. Compared to the model group, the AUC of the time-blood glucose curve showed a decreasing trend in the FLPs drug administration groups, indicating that FLPs accelerated glucose metabolism to reduce the blood glucose levels after intragastric administration of glucose (Fig. 2).

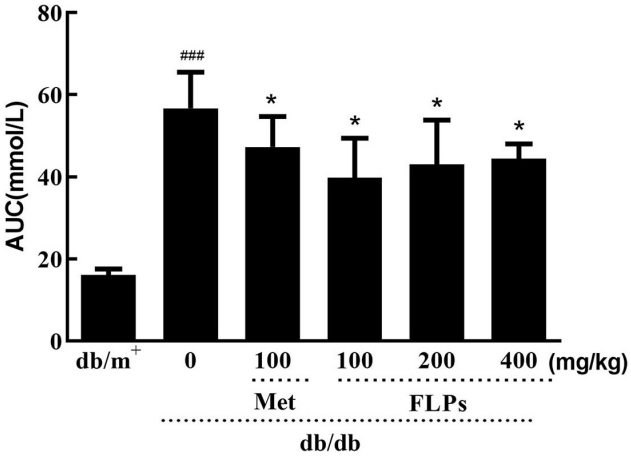

Fig. 2. The AUC changes of oral glucose tolerance of db/db mice. $^{###}p < 0.001$ versus db/m+ mice,$^{*}p < 0.05$ versus non-treated db/db mice.

3.3 Effects of FLPs on Blood Lipid Metabolism in db/db Mice

Type 2 DM is usually accompanied by abnormal blood lipid metabolism, usually manifesting as significantly increased levels of LDL-C, TG, and TC, and significantly decreased levels of HDL-C [34]. The results showed that compared with db/m+ group, the serum TC and TG values of the db/db model group increased, while the HDL-C values decreased indicating that db/db mice had significant serum lipid metabolism abnormalities. After the administration of FLPs, serum TG and TC levels decreased significantly ($p < 0.05$) (Fig. 3a,b). The FLPs (200 mg/kg) drug administration group exhibited increased HDL-C levels; however, the increase was not significant (Fig. 3c). These results indicated that FLPs reduced TC and TG; however, the effects on LDL-C and HDL-C were not significant.

3.4 Effects of FLPs on the Antioxidant Ability of Mice

Oxidative stress is the unifying pathogenesis with respect to complications in DM. If the ability to clear ROS and RNS is weak, resulting a lack of homeostasis, a large amount of ROS will accumulate, causing cell injury. High blood glucose results in the excessive production of acetyl-

Table 2. Amino acids composition in FLPs.

Compounds	Contents (%)	Compounds	Contents (%)
Glutamic acid (Glu)	0.753	Lysine (Lys)	0.949
Aspartic acid (Asp)	0.674	Phenylalanine (Phe)	0.837
Glycine (Gly)	0.593	Arginine (Arg)	0.581
Serine (Ser)	0.386	Tyrosine (Tyr)	0.467
Alanine (Ala)	0.253	Leucine (Leu)	0.413
DL-Methionine (Met)	0.243	Isoleucine (Iso)	0.298
Valine (Val)	0.198	Histidine (His)	0.205
L-Threonine (Thr)	0.116	Proline (Pro)	0.180

Table 3. The composition and percentage content of fatty acids in FLPs.

Compounds	Contents (‰)	Compounds	Contents (‰)	Compounds	Contents (‰)
Capric acid (C10:0)	0.45	Heptadecenoic acid (C17:1n7)	ND②	Arachidonic acid (C20:4n6)	2.48
Heptadecanoic acide (C17:0)	1.02	Arachidic acid (C20:0)	ND②	Docosadienoic acid (C22:2n6)	ND②
Hexadecanoic acid (C16:0)	35.97	Eicosadienoic acid (C20:2)	0.04	Docosahexaenoic acid (C22:6n3)	ND②
Lauric acid (C12:0)	ND②	Eicosaenoic acid (C20:1)	ND②	Docosanoic acide (C22:0)	ND②
Myristic acid (C14:0)	ND②	Heneicosanoic acid (C21:0)	ND②	Eicosapentaenoic acid (C20:5n3)	1.37
Myristoleic acid (C14:1n5)	ND②	Linoleic acid (C18:2n6c)	25.47	Eicosatrienoic acid (C20:3n3)	1.27
Octoic acid (C8:0)	ND②	Oleic acid (C18:1n9)	43.5	Eicosatrienoic acid (C20:3n6)	1.25
Palmitoleic acid (C16:1n7)	ND②	Stearic acid (C18:0)	13.19	Erucic acid (C22:1n9)	ND②
Pentadecanoic acid (C15:0)	0.33	Trans-linoleic acid (C18:2n6t)	ND②	Nervonic acid (C24:1n9)	ND②
Pentadecenoic acid (C15:1n5)	ND②	Trans-oleic acid (C18:1n9t)	3.69	Tetracosanoic acid (C24:0)	ND②
Tridecanoic acide (C13:0)	ND②	α-linolenic acid (C183n3)	ND②	Tricosanoic acid (C23:0)	ND②
Undecanoic acid (C11:0)	ND②	γ-linolenic acid (C18:3n6)	ND②		

ND②: not detected at the detection limit of 0.05 mg/kg.

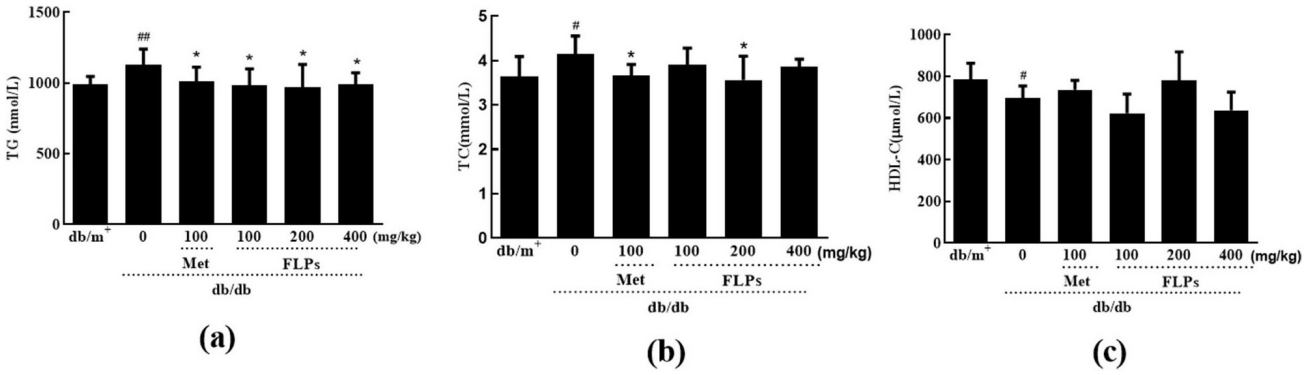

Fig. 3. Effects of FLPs on blood lipid metabolism in db/db mice. (a) The serum levels of TG; (b) the serum levels of TC, and (c) the serum levels of HDL-C in db/db mice compared to db/m+ mice. $^{\#}p < 0.05$ and $^{\#\#}p < 0.01$ versus db/m+ mice; $^{*}p < 0.05$ versus non-treated db/db mice.

CoA to produce more ROS and promote the progression of complications such as DM and DN [35,36]. CAT is expressed in many tissues, such as serum, kidney and liver, and catalyzes the conversion of H_2O_2 into H_2O and O_2 to alleviate oxidative stress injury [37]. GSH-Px and SOD are also antioxidative stress enzymes; and function to clear free radicals such as H_2O_2 and O_2^- [38].

3.4.1 Effects of FLPs on the Serum Antioxidant Ability of Mice

Compared with untreated db/db mice, in db/db mice, the serum CAT and GSH-Px values were increased after administration with 200 mg/kg FLPs (Fig. 4a,b), and the serum SOD values were increased after administered with 100 mg/kg and 400 mg/kg FLPs ($p < 0.01$, Fig. 4c).

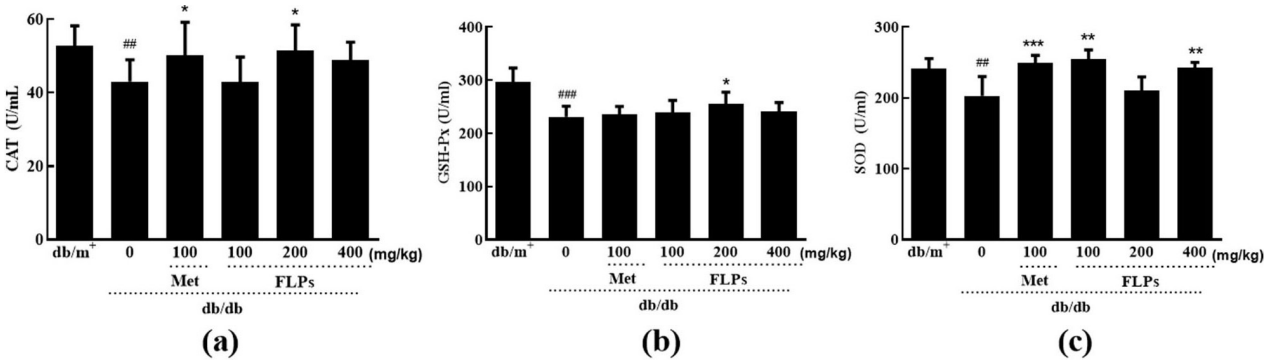

Fig. 4. Effects of FLPs on the Serum Antioxidant Ability of Mice. (a) The serum levels of CAT; (b) the serum levels of GSH-Px, and (c) the serum levels of SOD in db/db mice compared to db/m+ mice. $^{\#\#}p < 0.01$ and $^{\#\#\#}p < 0.001$ versus db/m+ mice; $*p < 0.05$, $**p < 0.01$ and $***p < 0.001$ versus non-treated db/db mice.

Table 4. Percentage composition of minerals (including heavy metals) in FLPs.

Compounds	Contents (‰)	Compounds	Contents (mg/kg)
Kalium (K)	137.10	Cuprum (Cu)	43.14
Natrium (Na)	2.57	Arsenic (As)	ND⑥
Calcium (Ca)	20.86	Mercury (Hg)	ND⑤
Ferrum (Fe)	0.30	Lead (Pb)	ND④
Zinc (Zn)	0.17		
Selenium (Se)	ND③		
Manganece (Mn)	0.03		
Chromium (Cr)	0.002		

ND③: not detected at the detection limit of 5 mg/kg.
ND④: not detected at the detection limit of 2 mg/kg.
ND⑤: not detected at the detection limit of 3 mg/kg.
ND⑥: not detected at the detection limit of 1 mg/kg.

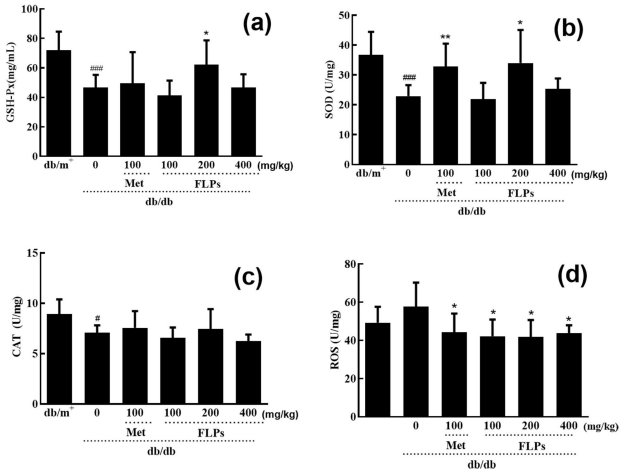

Fig. 5. Effects of FLPs on the Kidney Antioxidant Ability in Mice. (a) GSH-Px, (b) SOD, (c) CAT, and (d) ROS in the kidney of db/db mice compared to db/m+ mice. $^{\#}p < 0.05$ and $^{\#\#\#}p < 0.001$ versus db/m+ mice; $*p < 0.05$ and $**p < 0.01$ versus non-treated db/db mice.

3.4.2 Effects of FLPs on the Kidney Antioxidant Ability in Mice

Compared with untreated db/db mice, the values of GSH-Px and SOD in the kidney were significantly increased in db/db mice administered with 200 mg/kg FLPs ($p < 0.05$, Fig. 5a,b); CAT levels were slightly increased, but the increase was not significant (Fig. 5c). Compared with db/m+ mice, the ROS level in kidney tissues of untreated db/db mice increased, but not significantly. In addition, significant inhibitory effects on ROS levels were observed in the FLPs groups (Fig. 5d).

3.5 Effects of FLPs on Kidney Inflammation

More and more evidence indicated that type 2 DM is an inflammatory disease. The low-grade inflammation in DN is different from classic inflammation and is often referred to as microinflammation. Many cytokines are closely related to the occurrence and progression of type 2 DM and its complications [39–41]. The levels of cytokines and inflammatory factors, i.e., TNF-α, IFN-γ, IFN-α, IL-2, IL-6, IL-1β, N-acetylglutamate (NAG), MMP-9, and NF-κB, in kidney tissue were detected using ELISAs. The results indicated that compared to those in the model group, the levels of IL-2 and NAG in all groups administered FLPs were significantly decreased ($p < 0.001$, Fig. 6a,b). In the FLPs group (200 mg/kg), the levels of IFN-α and IFN-γ were significantly increased ($p < 0.01$, Fig. 6c,d), with no significant effects on IL-6, MMP-9, IL-1β, TNF-α, and NF- κB. Staining of kidney tissue in db/db mice exhibited pathological changes in comparison to db/m+ mice, such as glomerular hypertrophy, dilation of the glomerular capillaries, inflammatory cell infiltration, and basement membrane thickening of renal tubular epithelial cells. After FLPs administration, these pathological changes in kidney tissues improved, and protective functions of the kidney were restored (Fig. 7). These results indicated that FLPs had certain inhibitory functions on some inflammatory factors in kidney tissue, enhanced immune functions, and alleviated the progression of DN complications.

Table 5. Effects of 8-week FLPs treatments on weights, organ indexes and plasma glucose of mice.

	week	control	model	100 mg/kg Met	100 mg/kg FLPs	200 mg/kg FLPs	400 mg/kg FLPs
Body weights (g)	1	20.5 ± 1.5	40.9 ± 3.9$^{\#\#\#}$	43.0 ± 3.5	39.7 ± 2.4	42.6 ± 3.9	42.2 ± 3.7
	3	21.1 ± 1.5	43.7 ± 4.5$^{\#\#\#}$	45.0 ± 4.1	41.1 ± 2.9	45.6 ± 3.6	42.2 ± 3.6
	5	21.0 ± 1.5	47.3 ± 4.9$^{\#\#\#}$	43.2 ± 3.3*	41.8 ± 4.6*	46.8 ± 4.3	46.2 ± 4.8
	7	21.9 ± 1.3	50.8 ± 4.8$^{\#\#\#}$	48.0 ± 4.6	43.0 ± 7.6*	49.7 ± 5.1	48.3 ± 6.2
	9	20.7 ± 3.2	53.6 ± 4.9$^{\#\#\#}$	50.6 ± 7.3	44.3 ± 8.1**	53.4 ± 5.2	48.5 ± 6.9
Plasma glucose (mmol/L)	1	5.7 ± 1.3	18.3 ± 5.9$^{\#\#\#}$	18.0 ± 5.8	19.1 ± 5.6	17.4 ± 3.4	20.7 ± 5.4
	3	6.7 ± 1.5	18.7 ± 6.1$^{\#\#\#}$	18.4 ± 6.9	18.6 ± 5.7	16.1 ± 5.1	21.8 ± 6.0
	5	6.5 ± 1.1	18.1 ± 5.3$^{\#\#\#}$	17.8 ± 5.8	21.1 ± 7.9	17.6 ± 6.8	21.2 ± 4.3
	7	6.7 ± 1.6	21.6 ± 5.9$^{\#\#\#}$	16.0 ± 3.5*	17.9 ± 6.4	14.8 ± 3.3*	19.3 ± 2.9
	9	6.4 ± 2.5	20.4 ± 5.7$^{\#\#\#}$	13.4 ± 5.6*	17.7 ± 7.1	13.1 ± 3.2*	20.6 ± 5.4
organ indexs (g)	Liver	41.89 ± 2.5	60.29 ± 9.1$^{\#\#\#}$	64.43 ± 12.4	68.49 ± 9.7	66.93 ± 2.1	69.10 ± 24.9
	Spleen	3.07 ± 0.6	1.48 ± 0.5$^{\#\#\#}$	1.32 ± 0.2	1.27 ± 0.3	1.96 ± 1.4	1.34 ± 0.3
	Kidney	12.92 ± 0.6	7.37 ± 1.0$^{\#\#\#}$	7.02 ± 2.2	10.40 ± 4.1*	8.36 ± 1.5	9.73 ± 3.4*

The data were analyzed by one-way ANOVA and were expressed as means ± SD. $^{\#\#\#}p < 0.001$ versus db/m+ mice; $^{*}p < 0.05$ and $^{**}p < 0.01$ versus non-treated db/db mice.

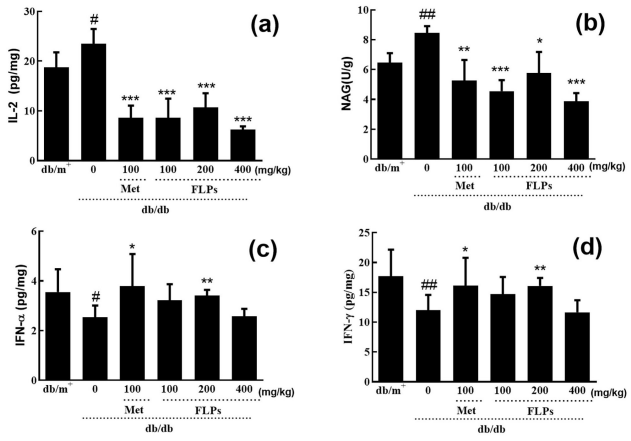

Fig. 6. Effects of FLPs on Kidney Inflammation. The levels of IL-2 (a), NAG (b), IFN-α (c), and IFN-γ (d) in the kidney of db/db mice compared to db/m+ mice. $^{\#}p < 0.05$ and $^{\#\#}p < 0.01$ versus db/m+ mice; * $p < 0.05$, **$p < 0.01$ and ***$p < 0.001$ versus non-treated db/db mice.

3.6 Regulation of FLPs on NRF2 Signal in Kidney

The potential mechanism of action of FLPs in DN was investigated using western blots. Compared to those in db/m+ mice, the expression levels of phosphorylated GSK-3β and mTOR protein in kidney tissue of db/db mice significantly increased, while the expression levels of CAT, HO-1, and NRF2 protein were significantly decreased ($p < 0.01$, $p < 0.001$). After FLPs administration, compared with the db/db model group, the expression levels of GSK-3β and mTOR aprotein significantly decreased, and all FLPs groups showed significant upregulation of NRF2 protein expression in the kidney of db/db mice. In addition, the levels of the antioxidases CAT and HO-1 in kidney tissue significantly increased ($p < 0.01$, Fig. 8). These results showed that FLPs targeted and regulated GSK-3β to further regulate the Keap1-independent nuclear factor erythroid 2-related factor 2/heme oxygenase 1 (NRF2/HO-1) signaling pathway to play an antioxidative and antiinflammatory role.

4. Discussion

This study used the spontaneously obese diabetic db/db mouse model to investigate therapeutic functions and mechanisms of action of FLPs in DN. The results indicated that FLPs inhibited excessive increases in mouse body weight, alleviated obesity symptoms in db/db mice to some extent, improved blood glucose control, and reduced DN changes in db/db mice. In addition FLPs did not cause toxic side effects, since changes in organ indicators were not significant. A significant improvement in oral glucose tolerance was observed in db/db mice when FLPs were administered. More than half of DM patients will develop lipid metabolism disorders that promote glomerulosclerosis and pathological changes related to DN. The main presentations are hypertriglyceridemia, increased LDL-C, and reduced HDL-C, eventually resulting in inflammatory factor release, resulting in proteinuria, kidney injury and kidney dysfunction. Experimental results showed that FLPs had significant inhibitory functions on TC and TG; therefore, they had certain blood lipid-lowering functions.

Increasing evidence indicates that the activities of many antioxidases in the body of DM patients decrease and that the redox status is imbalanced, thus producing oxidative stress [42,43]. In this study, the effects of FLPs on the activities of CAT, GSH-Px and SOD in the serum and kidney of mice were studied. The results showed that FLPs significantly increased the activities of these enzymes, reduced ROS production in kidney tissue, enhanced antioxidant activity in the body, and reduced oxidative stress and kidney injury.

Several studies have indicated that DN is an inflam-

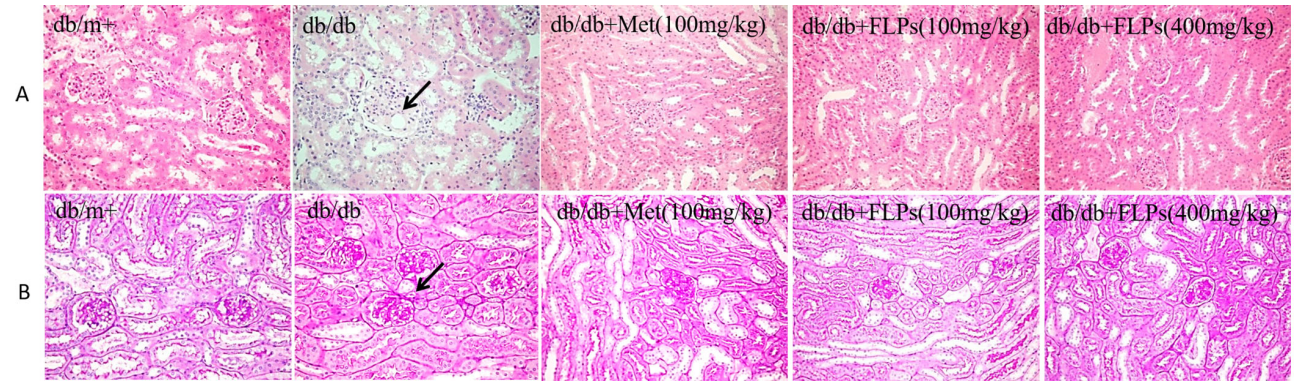

Fig. 7. The histopathological examination of kidney (A: H&E staining × 200, B: PAS staining × 200).

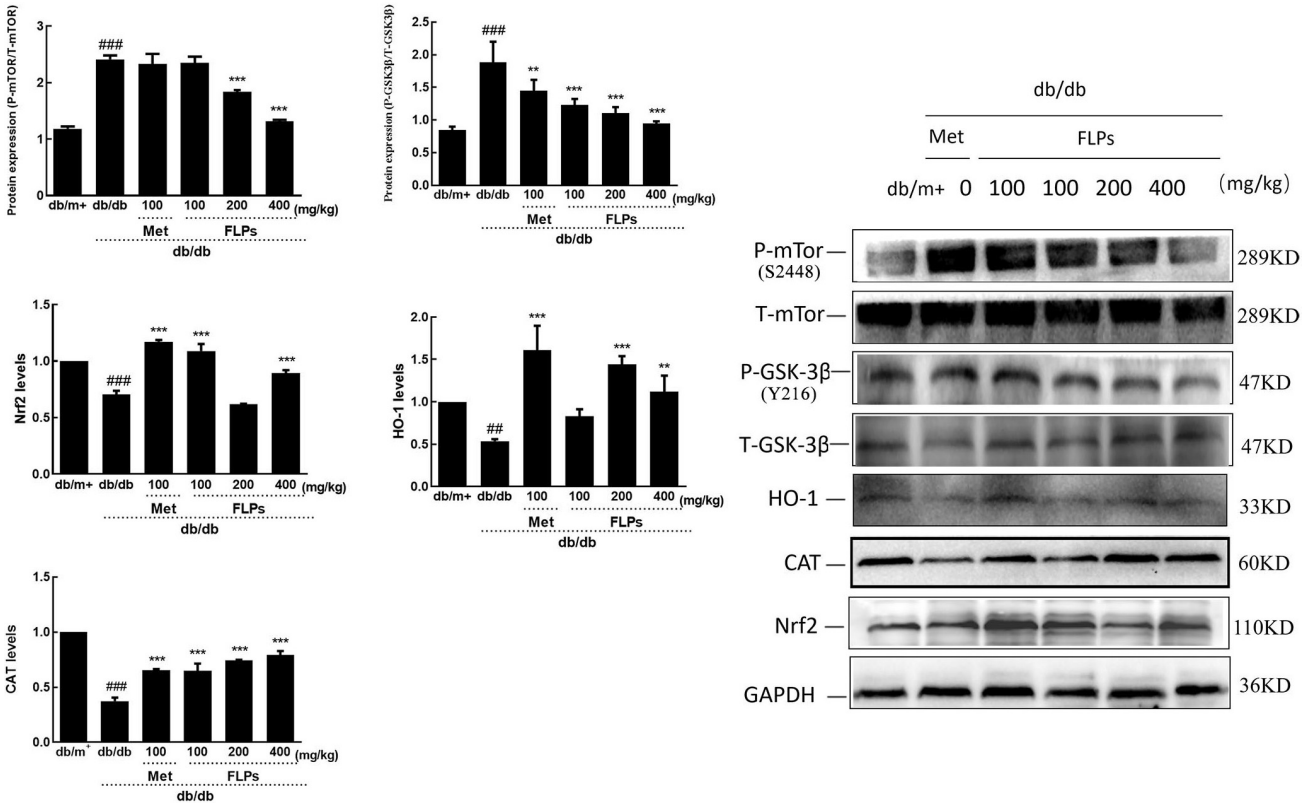

Fig. 8. FLPs treatment regulated the expressions of P-mTor, P-GSK3β, HO-1, CAT and NRF2 in kidney. The data of quantitative protein expression were standardized to the levels of GAPDH and related total proteins. $^{\#\#}p < 0.01$ and $^{\#\#\#}p < 0.001$ versus db/m+ mice; $^{**}p < 0.01$ and $^{***}p < 0.001$ versus nontreated db/db mice.

matory disease (microinflammation) and is different from classic inflammation. In a high-glucose environment, many cytokines and inflammatory factors are involved in the occurrence and development of DN. mTOR (PIKK) is an important substrate of AKT (protein kinase B, PKB). mTOR regulates many cellular functions and plays a critical role in DM, obesity, inflammation, tumors, and cardiovascular disease [44]. In addition, some studies have shown that the AMPK/mTOR signaling pathway can regulate the homeostasis imbalance of autophag y in the kidney. In DN, hyperglycemia and advanced glycation end products can inhibit the AMPK/mTOR signal transduction pathway, down-regulate autophagy, and accelerate the development of DN progression. This process provides a reference to further study the mechanism of the purified polysaccharide of FLPs on DN in the future. High blood glucose, vascular endothelial growth factor (VEGF), connective tissue growth factor (CTGF), and transforming growth factor beta 1 (TGF- β1) can all participate in the activation of the PI3K/AKT signaling pathway and subsequent development of DN complications such as renal interstitial fibrosis and mesangial cell hyperplasia and hypertrophy. GSK-3β is an extensively expressed serine/threonine kinase. GSK-3β is closely associated with the occurrence and develop-

ment of type 2 DM. With the administration of insulin, it participates in the regulation of glycogen synthase activity. It is associated with lipid metabolism regulation and participates in many signaling pathways including the AKT/GSK-3β/mTOR pathway [45,46]. This study demonstrated that FLPs administration effectively regulated the expression of mTOR and GSK-3β and activated NRF2. Oxidative stress and inflammation caused kidney tissue injury, which was alleviated by upregulating HO-1 and CAT.

5. Conclusions

This study demonstrated the protective function of FLPs against oxidative stress in DM and DN complications and confirmed that FLPs negatively regulated NRF2 by inhibiting of GSK-3β activity to activate the NRF2/HO-1 pathway for the first time.

Availability of Data and Materials

All data generated or analyzed during this study are included in this published article.

Author Contributions

HW, DL and YL designed the research study. HW and YY performed the research. SW, CL and CC provided help and advice on the research. HW and XW analyzed the data. HW and YY wrote the manuscript. All authors contributed to editorial changes in the manuscript. All authors read and approved the final manuscript.

Ethics Approval and Consent to Participate

All animal experiments were performed strictly according to the regulations for the use of experimental animals and the Animal Welfare Law of China and approved by Animal Experimental Ethical Inspection Form of Changchun University of Chinese Medicine (Approval No. 20190036).

Acknowledgment

The authors thank Prof. Di Wang of Jilin Agricultural University for providing advice on the research.

Funding

This research was funded by the National Key Research and Development Program of China (No. 2021YFD1600401), Jilin Province Science and Technology Development Plan Project (No. 20210401121YY), Central Public-interest Scientific Institution Basal Research Fund (No. 1630042022003), the Strategic Priority Research Program of the Chinese Academy of Sciences (XDA28080300), China Agriculture Research System, grant number CARS-20, and the Hainan Provincial Natural Science Foundation of China (No. 322QN365).

Conflict of Interest

The authors declare no conflict of interest.

References

[1] Johnstone MT, Veves A. Diabetes and Cardiovascular Disease. 2nd edn. Humana Press: Totowa, USA. 2005.

[2] Boyle JP, Thompson TJ, Gregg EW, Barker LE, Williamson DF. Projection of the year 2050 burden of diabetes in the US adult population: dynamic modeling of incidence, mortality, and prediabetes prevalence. Population Health Metrics. 2010; 8: 29.

[3] Yang W, Lu J, Weng J, Jia W, Ji L, Xiao J, *et al*. Prevalence of diabetes among men and women in China. The New England Journal of Medicine. 2010; 362: 1090–1101.

[4] Hanna FW, Duff CJ, Shelley-Hitchen A, Hodgson E, Fryer AA. Diagnosing gestational diabetes mellitus: implications of recent changes in diagnostic criteria and role of glycated haemoglobin (HbA1c). Clinical Medicine. 2017; 17: 108–113.

[5] Gray SP, Cooper ME. Diabetic nephropathy in 2010: Alleviating the burden of diabetic nephropathy. Nature Reviews Nephrology. 2011; 7: 71–73.

[6] Hadjadj S, Cariou B, Fumeron F, Gand E, Charpentier G, Roussel R, *et al*. Death, end-stage renal disease and renal function decline in patients with diabetic nephropathy in French cohorts of type 1 and type 2 diabetes. Diabetologia. 2016; 59: 208–216.

[7] Ruiz S, Pergola PE, Zager RA, Vaziri ND. Targeting the transcription factor Nrf2 to ameliorate oxidative stress and inflammation in chronic kidney disease. Kidney International. 2013; 83: 1029–1041.

[8] Jiang Y, Bao H, Ge Y, Tang W, Cheng D, Luo K, *et al*. Therapeutic targeting of GSK3β enhances the Nrf2 antioxidant response and confers hepatic cytoprotection in hepatitis C. Gut. 2015; 64: 168–179.

[9] Correa F, Mallard C, Nilsson M, Sandberg M. Activated microglia decrease histone acetylation and Nrf2-inducible antioxidant defence in astrocytes: restoring effects of inhibitors of HDACs, p38 MAPK and GSK3β. Neurobiology of Disease. 2011; 44: 142–151.

[10] Kanninen K, White AR, Koistinaho J, Malm T. Targeting Glycogen Synthase Kinase-3β for Therapeutic Benefit against Oxidative Stress in Alzheimer's Disease: Involvement of the Nrf2-ARE Pathway. International Journal of Alzheimer's Disease. 2011; 2011: 985085.

[11] Copple IM. The Keap1-Nrf2 cell defense pathway-a promising therapeutic target? Advances in Pharmacology. 2012; 63: 43–79.

[12] Landis RC, Quimby KR, Greenidge AR. M1/M2 Macrophages in Diabetic Nephropathy: Nrf2/HO-1 as Therapeutic Targets. Current Pharmaceutical Design. 2018; 24: 2241–2249.

[13] Bao L, Li J, Zha D, Zhang L, Gao P, Yao T, *et al*. Chlorogenic acid prevents diabetic nephropathy by inhibiting oxidative stress and inflammation through modulation of the Nrf2/HO-1 and NF-κB pathways. International Immunopharmacology. 2018; 54: 245–253.

[14] Nabavi SF, Barber AJ, Spagnuolo C, Russo GL, Daglia M, Nabavi SM, *et al*. Nrf2 as molecular target for polyphenols: A novel therapeutic strategy in diabetic retinopathy. Critical Reviews in Clinical Laboratory Sciences. 2016; 53: 293–312.

[15] Ruthes AC, Smiderle FR, Iacomini M. Mushroom heteropolysaccharides: A review on their sources, structure and biological effects. Carbohydrate Polymers. 2016; 136: 358–375.

[16] Friedman M. Mushroom Polysaccharides: Chemistry and Antiobesity, Antidiabetes, Anticancer, and Antibiotic Properties in Cells, Rodents, and Humans. Foods. 2016; 5: 80.

[17] Pouzar Z. Nova genera macromycetum I. Ceská Mykologie. 1957; 11: 48–50.

[18] Li Y, Li TH, Yang ZL, Bau T, Dai YC. Atlas of Chinese macrofungal resources. Zhongyuan Farmers' Press: Zhengzhou, China. 2015. (In Chinese)
[19] Xie ZL, Zhao LZ, Li Y, Lei JQ, Zhang FM. The correlation of geographic distribution and ecological environment of endemic species Floccularia luteovirenson Qinghai-Tibet Plateau. Acta Ecologica Sinica. 2016; 36: 2851–2857.
[20] Xing R, Gao QB, Zhang FQ, Fu PC, Wang JL, Yan HY, *et al*. Genetic variation and phylogenetic relationships of the ectomycorrhizal Floccularia luteovirens on the Qinghai-Tibet Plateau. Journal of Microbiology. 2017; 55: 600–606.
[21] Wang H, Wang SM, Chen CB, Li Y. Assessment of antioxidant and anti-inflammatory potential of the aqueous extract of Floccularia luteovirens in diabetic rats. Mycosystema. 2019; 38: 1519–1526.
[22] Wang H, Chen CB, Zhang B, Tong XD, Wang SM, Li Y. Antioxidant activities and extraction technique optimization of crude polysaccharides from the fruiting body of Floccularia luteovirens. Mycosystema. 2019; 38: 1681–1688.
[23] Yan JK, Li L, Wang ZM, Wu JY. Structural elucidation of an exopolysaccharide from mycelial fermentation of a Tolypocladium sp. fungus isolated from wild Cordyceps sinensis. Carbohydrate Polymers. 2010; 79: 125–130.
[24] Chen BJ, Shi MJ, Cui S, Hao SX, Hider RC, Zhou T. Improved antioxidant and anti-tyrosinase activity of polysaccharide from Sargassum fusiforme by degradation. International Journal of Biological Macromolecules. 2016; 92: 715–722.
[25] DuBois M, Gilles KA, Hamilton JK, Rebers PA, Smith F. Colorimetric method for determination of sugars and related substances. Analytical Chemistry. 1956; 28: 350–356.
[26] Xue P, Zhao Y, Wen C, Cheng S, Lin S. Effects of electron beam irradiation on physicochemical properties of corn flour and improvement of the gelatinization inhibition. Food Chemistry. 2017; 233: 467–475.
[27] Wang H, Pampati N, McCormick WM, Bhattacharyya L. Protein Nitrogen Determination by Kjeldahl Digestion and Ion Chromatography. Journal of Pharmaceutical Sciences. 2016; 105: 1851–1857.
[28] Zhao C, Zhao X, Zhang J, Zou W, Zhang Y, Li L, *et al*. Screening of Bacillus Strains from Sun Vinegar for Efficient Production of Flavonoid and Phenol. Indian Journal of Microbiology. 2016; 56: 498–503.
[29] Liu Y, Li L, An S, Zhang Y, Feng S, Zhao L, *et al*. Antifatigue Effects of Antrodia cinnamomea Cultured Mycelium via Modulation of Oxidative Stress Signaling in a Mouse Model. BioMed Research International. 2017; 2017: 9374026.
[30] Wang X, Qu Y, Zhang Y, Li S, Sun Y, Chen Z, *et al*. Antifatigue Potential Activity of Sarcodon imbricatus in Acute Excise-Treated and Chronic Fatigue Syndrome in Mice via Regulation of Nrf2-Mediated Oxidative Stress. Oxidative Medicine and Cellular Longevity. 2018; 2018: 9140896.
[31] Falandysz J, Szymczyk K, Ichihashi H, Bielawski L, Gucia M, Frankowska A, *et al*. ICP/MS and ICP/AES elemental analysis (38 elements) of edible wild mushrooms growing in Poland. Food Additives and Contaminants. 2001; 18: 503–513.
[32] Subramanian R, Asmawi MZ, Sadikun A. In vitro alpha-glucosidase and alpha-amylase enzyme inhibitory effects of Andrographis paniculata extract and andrographolide. Acta Biochimica Polonica. 2008; 55: 391–398.
[33] Ahuja V, Aronen P, Pramodkumar TA, Looker H, Chetrit A, Bloigu AH, *et al*. Accuracy of 1-Hour Plasma Glucose During the Oral Glucose Tolerance Test in Diagnosis of Type 2 Diabetes in Adults: A Meta-analysis. Diabetes Care. 2021; 44: 1062–1069.
[34] Tsumura M, Kinouchi T, Ono S, Nakajima T, Komoda T. Serum lipid metabolism abnormalities and change in lipoprotein contents in patients with advanced-stage renal disease. Clinica Chimica Acta. 2001; 314: 27–37.
[35] Kashihara N, Haruna Y, Kondeti VK, Kanwar YS. Oxidative stress in diabetic nephropathy. Current Medicinal Chemistry. 2010; 17: 4256–4269.
[36] Yan LJ. Pathogenesis of chronic hyperglycemia: from reductive stress to oxidative stress. Journal of Diabetes Research. 2014; 2014: 137919.
[37] Dinçer Y, Telci A, Kayali R, Yilmaz IA, Cakatay U, Akçay T. Effect of alpha-lipoic acid on lipid peroxidation and antioxidant enzyme activities in diabetic rats. Clinical and Experimental Pharmacology & Physiology. 2002; 29: 281–284.
[38] Brownlee M. The pathobiology of diabetic complications: a unifying mechanism. Diabetes. 2005; 54: 1615–1625.
[39] Cavallo MG, Pozzilli P, Bird C, Wadhwa M, Meager A, Visalli N, *et al*. Cytokines in sera from insulin-dependent diabetic patients at diagnosis. Clinical and Experimental Immunology. 1991; 86: 256–259.
[40] Anders HJ, Ryu M. Renal microenvironments and macrophage phenotypes determine progression or resolution of renal inflammation and fibrosis. Kidney International. 2011; 80: 915–925.
[41] Wada J, Makino H. Inflammation and the pathogenesis of diabetic nephropathy. Clinical Science. 2013; 124: 139–152.
[42] Lee HB, Yu MR, Yang Y, Jiang Z, Ha H. Reactive oxygen species-regulated signaling pathways in diabetic nephropathy. Journal of the American Society of Nephrology. 2003; 14: S241–S245.
[43] Evans JL, Goldfine ID, Maddux BA, Grodsky GM. Are oxidative stress-activated signaling pathways mediators of insulin resistance and beta-cell dysfunction? Diabetes. 2003; 52: 1–8.
[44] Weichhart T, Säemann MD. The multiple facets of mTOR in immunity. Trends in Immunology. 2009; 30: 218–226.
[45] Xu G, Zhao X, Fu J, Wang X. Resveratrol increase myocardial Nrf2 expression in type 2 diabetic rats and alleviate myocardial ischemia/reperfusion injury (MIRI). Annals of Palliative Medicine. 2019; 8: 565–575.
[46] Liang X, Wang P, Chen B, Ge Y, Gong AY, Flickinger B, *et al*. Glycogen synthase kinase 3β hyperactivity in urinary exfoliated cells predicts progression of diabetic kidney disease. Kidney International. 2020; 97: 175–192.